Lifetime measurement of the 8*s* level in francium

E. Gomez,[1] L. A. Orozco,[2] A. Perez Galvan,[2] and G. D. Sprouse[1]
[1]*Department of Physics and Astronomy, SUNY Stony Brook, Stony Brook, New York 11794-3800, USA*
[2]*Department of Physics, University of Maryland, College Park, Maryland 20742-4111, USA*
(Received 22 February 2005; published 22 June 2005)

We measure the lifetime of the 8*s* level of ^{210}Fr atoms on a magneto-optically trapped sample with time-correlated single-photon counting. The $7P_{1/2}$ state serves as the resonant intermediate level for two-step excitation of the 8*s* level completed with a 1.3-μm laser. Analysis of the fluorescence decay through the $7P_{3/2}$ level gives 53.30 ± 0.44 ns for the 8*s* level lifetime.

DOI: 10.1103/PhysRevA.71.062504 PACS number(s): 32.70.Cs, 32.10.Dk, 32.80.Pj

We present in this paper a measurement of the 8*s* level lifetime of francium, the heaviest of alkali-metal atoms. Fr is yet to be used in parity nonconservation (PNC) measurements [1], but work toward that goal requires understanding of the excited-state properties of the atom. The 8*s* state is the preferred candidate for an optical PNC measurement; the dipole-forbidden excitation between the $7S_{1/2}$ ground state and the first excited $8S_{1/2}$ state becomes allowed through the weak interaction. The equivalent state in Cs (7*s*) has been used in PNC experiments by the Boulder [2,3] and Paris [4] groups and a quantitative understanding of this state—its lifetime and its branching ratio—is critical to the successful extraction of weak-interaction physics in these experiments.

Our measurement is a test of the modern techniques of *ab initio* calculations using many-body perturbation theory (MBPT) [5,6]. Quantitative measurements on Fr and comparison with theoretical calculations validate the same MBPT techniques used for Cs and other atoms with a more relativistic atom where correlations from the 87 electrons are large.

The lifetime τ of an excited state is determined by its individual decay rates $1/\tau_i$ through the matrix element associated with the *i* partial decay rate. The connections between lifetime, partial decay rates, and matrix elements are

$$\frac{1}{\tau} = \sum_i \frac{1}{\tau_i}, \tag{1}$$

$$\frac{1}{\tau_i} = \frac{4}{3}\frac{\omega^3}{c^2}\alpha\frac{|\langle J\|r\|J'\rangle|^2}{2J'+1}, \tag{2}$$

where ω is the transition energy divided by $\hbar$, c is the speed of light, α is the fine-structure constant, J' and J are, respectively, the initial- and final-state angular momenta, and $|\langle J\|r\|J'\rangle|$ is the reduced matrix element [7]. Equation (2) links the lifetime of an excited state to the electronic wave functions of the atom. Comparisons of measurements with theoretical predictions test the quality of the computed wave functions especially at large distances from the nucleus due to the presence of the radial operator.

The lifetimes of the low-lying states in Fr are reaching a level of precision comparable to that of the other alkali metals [7–9]. The atomic theory calculations for these transitions [10–12] predict lifetimes measured with impressive agreement, strengthening the possibility of a PNC experiment in a chain of francium isotopes.

We use the method of time-correlated single-photon counting to obtain the lifetime of the 8*s* level in Fr in a magneto-optical trap (MOT). We populate the 8*s* level with a two-step excitation, and then we turn off the excitation suddenly and observe the exponential decay through the fluorescence photons [13].

The production, cooling, and trapping of Fr online with the superconducting linear accelerator at Stony Brook has been described previously [14]. Briefly, a 100-MeV beam of ^{18}O ions from the accelerator impinges on a gold target to make ^{210}Fr (radioactive half-life 3 min). We extract $\sim 1 \times 10^6$ francium ions/s out of the gold and transport them 15 m to a cold yttrium neutralizer where we accumulate the Fr atoms. We then close the trap with the neutralizer and heat it for one second ($\sim$1000 K) to release the atoms into the dry-film-coated glass cell where they are cooled and trapped in a MOT. The cycle of accumulating and trapping repeats every 20 s.

Figure 1 shows the states of ^{210}Fr relevant for trapping and lifetime measurements. The nuclear spin of this isotope

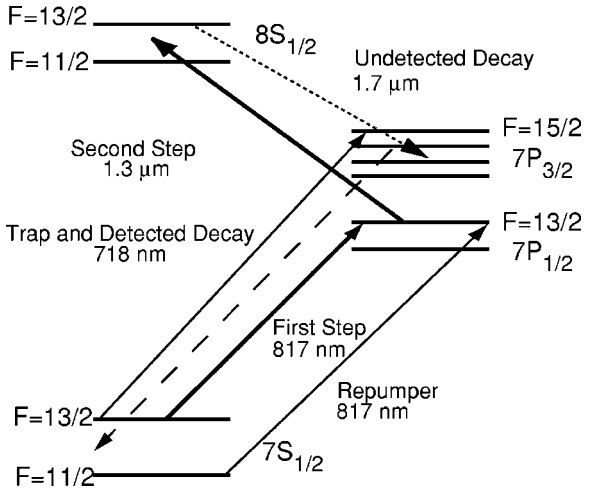

FIG. 1. Energy levels of ^{210}Fr. The figure shows the trapping and repumping transitions (thin solid lines), the two-step excitation (thick solid lines), the fluorescence detection used in the lifetime measurement (dashed line), and the undetected fluorescence (dotted line).

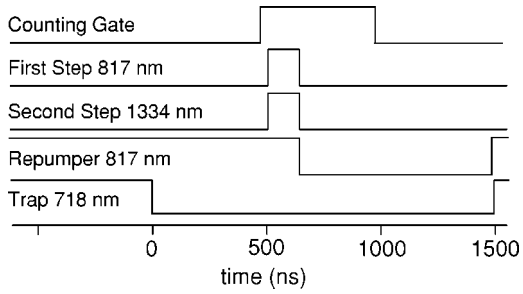

FIG. 2. Timing diagram for the 8*s* level excitation and decay cycle (100 kHz).

is $I=6$ with a ground-state hyperfine splitting of 46.768 GHz. A Coherent 899-21 titanium-sapphire (Ti:sapphire) laser operating at 718 nm excites the trapping and cooling transition ($7S_{1/2}$, $F=13/2 \rightarrow 7P_{3/2}$, $F=15/2$) (trap in Fig. 1). A Coherent 899-21 Ti:sapphire laser operating at 817 nm repumps any atoms that leak out of the cooling cycle via the $7S_{1/2}$, $F=11/2 \rightarrow 7P_{1/2}$, $F=13/2$ transition (repumper in Fig. 1). The first step for the $7S_{1/2} \rightarrow 8S_{1/2}$ excitation comes from a Coherent 899-01 Ti:Sapphire at 817 nm, it resonantly populates the $7P_{1/2}$, $F=13/2$ state (first step in Fig. 1). The second step at 1.3 μm originates from an EOSI 2010 diode laser to excite also resonantly the $7P_{1/2} \rightarrow 8S_{1/2}$ transition (second step in Fig. 1).

A Burleigh WA-1500 wavemeter monitors the wavelength of all lasers to about ± 0.001 cm^{-1}. We lock the trap, first step, and repumper lasers with a transfer lock [15], while we lock the second step laser with the aid of a Michelson interferometer that is itself locked to the frequency-stabilized HeNe laser used in the transfer lock.

The MOT consists of three pairs of retroreflected beams, each with 15 mW/cm^2 intensity, 3 cm diameter ($1/e$ intensity), and red detuned 31 MHz from the atomic resonance. A pair of coils generates a magnetic field gradient of 9 G/cm. We work with traps of $\approx 10^4$ atoms, a temperature lower than 300 μK, with a diameter of 0.5 mm and a typical lifetime between 5 and 10 s.

Figure 2 displays the timing sequence for the excitation and decay cycle for the measurement. Both lasers of the two step excitation are on for 50 ns before they are switched off, while the counting electronics are sensitive for 500 ns to record the excitation and decay signal. The trap laser turns off 500 ns before the two-photon excitation. We repeat the cycle at 100 kHz.

We turn the trap light on and off with an electro-optic modulator (EOM) (Gsänger LM0202) and an acousto-optic modulator (AOM) (Crystal Technology 3200-144). The combination of the two gives an extinction ratio of better than 1600:1 after 500 ns. AOM's (Crystal Technology 3200) modulate the repumper (first step light) with extinction ratio of 109:1 (26:1) 30 ns after the pulse turns off. We couple the 1.3-μm laser into a single-mode optical fiber and pass it through a 10-Gbit/s lithium-niobate electro-optic fiber modulator (Lucent Technologies 2623N), then amplify it (Iphenix IPSAD1301), and again modulate it with a second electro-optic fiber modulator (Lucent Technologies 2623N); the result is an on-off ratio of better than 1000:1 in a time of 20 ns.

A 1:1 imaging system ($f/3.9$) collects the fluorescence photons onto a charge-coupled-device (CCD) camera (Roper Scientific, MicroMax 1300YHS-DIF). We monitor the trap with the use of an interference filter at 718 nm in front of the camera. A beam splitter in the imaging system sends 50% of the light onto a photomultiplier tube (PMT) (Hamamatsu R636). An interference filter at 718 nm in front of the PMT reduces the background light other than fluorescence from the cascade through the $7P_{3/2}$ level decay back to the ground state $7S_{1/2}$.

After we turn off the excitation lasers, the atom returns back to the ground level using two different decay channels: First, by emitting a 1.3-μm photon it decays back to the $7P_{1/2}$ state and fluoresces 817-nm light to return to the 7*s* ground level. The second possible decay channel is the 8*s* $\rightarrow 7P_{3/2}$ transition (dotted line in Fig. 1) followed by the decay to the 7*s* ground level (dashed line in Fig. 1). The 1.7-μm fluorescence from the first step of this decay is unobserved, but we detect 718-nm light from the second part of the decay. With the known lifetime of the $7P_{3/2}$ state, it is possible to extract the 8*s* level lifetime from the cascade fluorescence decay.

We amplify (Ortec AN106/N) the current pulses from the photon detections in the PMT. We gate (EG&G LG101/N) and send them to a constant fraction discriminator (Ortec 934). The output starts a gated time-to-amplitude converter (TAC) (Ortec 467), which we stop with a fixed-time-delay pulse after the two-photon excitation. We use a multichannel analyzer (MCA) (EG&G Trump-8k) to produce a histogram of the events showing directly the exponential decay. A pulse generator provides the primary timing sequence for the measurement (Berkeley Nucleonics Corporation BNC 8010).

We take sets of data for about 1500 s, which are individually processed and fitted. The total number of counts in a set is typically in the order of 3×10^5. Figure 3 shows the accumulated decay of a set of data, together with the exponential fit and the residuals.

We apply a pileup correction that accounts for the preferential counting of early events [16]. As low count rates keep this correction small, we collect data with a small number of fluorescence photons. We typically count one photon every 500 cycles. The correction alters the fitted lifetime by +0.1%. We perform a nonlinear least-squares fit and use an iterative algorithm to find the fitting parameters that produce the smallest χ^2.

The decay signal S_{8s} through the $7P_{3/2}$ state is a sum of two exponentials [9] and a background with a slope [see Eq. (3)]. There are two possible sources of light at 718 nm: cascade fluorescence from atoms excited to the 8*s* level and the remaining trapping light. The background with the slope in the fitting function term comes from the latter. It allows us to include the long-term response of the electro- and acousto-optic devices that turn off the trap light. It is a small contribution, but we have measured it and add it to the fitting function to obtain

$$S_{8s} = A_{8s} \exp\left(-\frac{t}{\tau_{8s}}\right) + A_{7p} \exp\left(-\frac{t}{\tau_{7p}}\right) + A_B + A_S t, \quad (3)$$

where τ_{7p} is the known lifetime of the $7P_{3/2}$ state and τ_{8s} the lifetime we want to extract. A_B and A_S characterize the back-

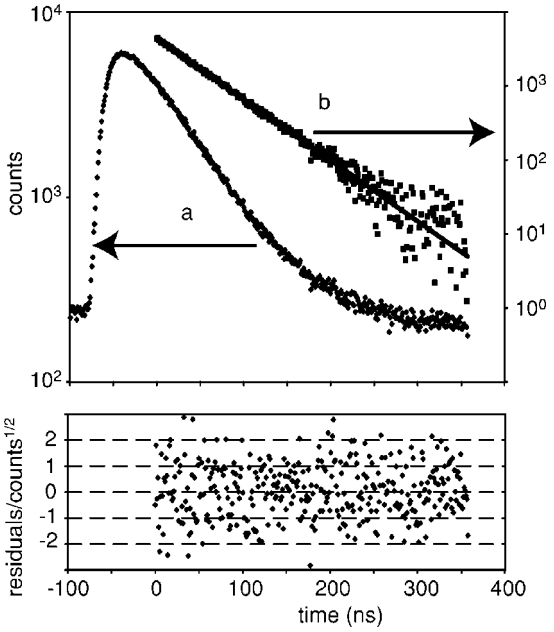

FIG. 3. Cascading decay curve of the 8*s* level through the $7P_{3/2}$ state with fit and residuals. *a* is the arrival time histogram data and *b* the data after the subtraction of the $7P_{3/2}$ decay and the background. The solid line is the fit. The lower plot shows the normalized residuals.

ground while A_{8s} and A_{7p} determine the amplitudes of the decaying exponentials.

Figure 3 shows an example of a data set and the fit. We start the fit 20 ns after both excitation lasers are turned off. The fitting function describes the data well, and the reduced χ^2_ν of this particular decay is 1.11. A discrete Fourier transform of the residuals shows no structure. The average χ^2_ν for all the data files used to obtain the lifetime is 1.07 ± 0.07. A change (within our quoted uncertainty) on the calibration of the linearity of the MCA is responsible for deviation from unity of the reduced χ^2. The slope that we find is 0.02 counts in 500 channels for a counting time of 1 s. A fit to a file consisting of the sum of all files gives consistent results both for the 8*s* lifetime and for the $7P_{3/2}$ lifetime when this last one is left as a free parameter.

We calculate the contribution to the uncertainty in the 8*s* lifetime from the $7P_{3/2}$ lifetime of 21.02(11) ns [8] using Bayesian statistics [9]. The $7P_{3/2}$ state gives a Bayesian error of 0.15%.

We do not observe any systematic effects depending on the start and end points of the fit, the so-called truncation error, beyond the statistical uncertainty. We look for effects in the lifetime from imperfect lasers turn off by leaving the first-step light on continuously. The change in the lifetime with the first-step light off or continuously on during the decay constraints the uncertainty from imperfect lasers turn off to ±0.07%. The time calibration of the pulse detection system contributes ±0.01% to the uncertainty. The TAC and MCA nonuniformities contribute ±0.11% error in the 8*s* level lifetime and increases the value of the χ^2_ν.

We study the effect of the initial state conditions on the obtained lifetime by changing external parameters of the measurement. We vary the power of the 817-nm first-step laser and we observe no change in the measured lifetime. The time of flight of the atoms can influence the measured 8*s* level as excited atoms may leave the imaging region before they fluoresce. However, the average velocity of the atoms in the MOT is less than 0.1 m/s and the imaging region has a diameter of 1 mm. The time it takes the atoms to traverse the imaging region is approximately 10^5 times the measured 8*s* level lifetime, so this is not an issue.

TABLE I. Error budget for the 8*s* level lifetime measurement.

	Error [%]
Time calibration	±0.01
Bayesian error	±0.15
TAC/MCA response nonuniformity	±0.11
Radiation trapping	±0.01
Imperfect laser turnoff	±0.07
Magnetic field	±0.11
Background slope	±0.36
PMT response	±0.24
Statistical error	±0.65
Total	±0.82

The slope in the fitting function influences the value of the obtained lifetime by less than 1%. We analyze files with and without the atomic decay but always with the trap light and they give a consistent slope. We compare the lifetime obtained by leaving the slope as a free parameter or by fixing it to the background files value and obtain an uncertainty contribution of ±0.36%.

The counting PMT is continuously on and detects light from both the two-step excitation and the fluorescence light

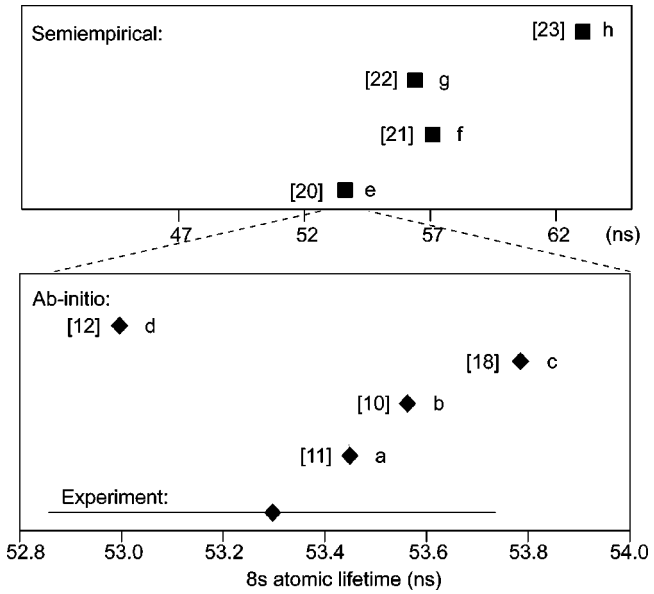

FIG. 4. Comparison of the 8*s* level lifetime with theory. The calculations are labeled with letters explained in the text and with numbers that indicate the reference.

from the MOT. We bound the possible saturation effects on the PMT by comparing the average response of the PMT in photon counting mode with the response of a fast photodiode not subject to saturation. We find a maximum contribution of ±0.24% to the overall uncertainty from the PMT recovery.

We search for other possible systematic effects in the lifetime of the equivalent level (6*s*) in Rb, given the complications of working with Fr. These measurements are performed both in a vapor cell and in a MOT. There can be collisional quenching or radiation trapping in a gas of atoms that can modify the lifetime; however, we find no evidence of change when we vary the number of atoms from 10^3 to 10^5 in the Rb trap and we establish a limit on radiation trapping from the Rb data of ±0.01%. We have performed an extensive search for some additional magnetic sensitivity: there is no change in the lifetime beyond the statistical uncertainty when we change the gradient of the Fr MOT. The detection of the cascaded photon reduces the possibility of quantum beats [13]. We establish a limit on magnetic field effects of ±0.11% in the uncertainty of the Fr measurement consistent with our work in Rb [17].

Table I contains the error budget for the 8*s* level lifetime measurement. The statistical error dominates the uncertainty of the measurement. We obtain a lifetime of 53.30 ± 0.44 ns for the 8*s* level of francium.

Figure 4 compares the obtained 8*s* level lifetime with theoretical calculations. *a*–*d* are *ab initio* MBPT calculations of the dipole matrix elements by *a* (Safronova *et al.* [11]), *b* (Dzuba *et al.* [10]), *c* (Johnson *et al.* [18]), and *d* (Dzuba *et al.* [12]). We calculate the lifetime with Eq. (2) from their predictions and measured transition energies [19]. *e*–*h* are semiempirical calculations: *e* (Marinescu *et al.* [20]), *f* (Theodosiou [21]), *g* (Biémont *et al.* [22]), and *h* (van Wijngaarden and Xia [23]). The scatter of results from the MBPT calculations is small and they are all within 1% of our result. The semiempirical methods are less accurate and they have a broader scatter for their predictions (expanded scale in Fig. 4).

In summary we have measured the lifetime of the 8*s* level of francium to a precision of 0.8%. Our measurement establishes that the MBPT calculations of matrix elements that contribute to the total lifetime of the state are very good. They take into account the large relativistic effects present in this heavy atom as well as the multiple correlations from its 87 electrons. Their accuracy is vital for future interpretations of PNC measurements. The agreement of theoretical predictions over different species reinforces the interpretation of PNC measurements in Cs which are now sensitive to the nuclear weak force [2].

Work supported by NSF. E.G. acknowledges support from CONACYT and the authors thank the personnel of the Nuclear Structure Laboratory at Stony Brook for their support as well as J. Gripp, J. E. Simsarian, and B. Minford for equipment loans.

[1] M.-A. Bouchiat and C. Bouchiat, Rep. Prog. Phys. **60**, 1351 (1997).
[2] C. S. Wood, S. C. Bennett, D. Cho, B. P. Masterson, J. L. Roberts, C. E. Tanner, and C. E. Wieman, Science **275**, 1759 (1997).
[3] C. S. Wood, S. C. Bennett, J. L. Roberts, D. Cho, and C. E. Wieman, Can. J. Phys. **77**, 7 (1999).
[4] J. Guéna, D. Chauvat, P. Jacquier, E. Jahier, M. Lintz, S. Sanguinetti, A. Wasan, M. A. Bouchiat, A. V. Papoyan, and D. Sarkisyan, Phys. Rev. Lett. **90**, 143001 (2003).
[5] W. R. Johnson, M. S. Safronova, and U. I. Safronova, Phys. Rev. A **67**, 062106 (2003).
[6] J. S. M. Ginges and V. V. Flambaum, Phys. Rep. **397**, 63 (2004).
[7] J. M. Grossman, R. P. Fliller III,, L. A. Orozco, M. R. Pearson, and G. D. Sprouse, Phys. Rev. A **62**, 062502 (2000).
[8] J. E. Simsarian, L. A. Orozco, G. D. Sprouse, and W. Z. Zhao, Phys. Rev. A **57**, 2448 (1998).
[9] S. Aubin, E. Gomez, L. A. Orozco, and G. D. Sprouse, Phys. Rev. A **70**, 042504 (2004).
[10] V. A. Dzuba, V. V. Flambaum, and O. P. Sushkov, Phys. Rev. A **51**, 3454 (1995).
[11] M. S. Safronova, W. R. Johnson, and A. Derevianko, Phys. Rev. A **60**, 4476 (1999).
[12] V. A. Dzuba, V. V. Flambaum, and J. S. M. Ginges, Phys. Rev. A **63**, 062101 (2001).
[13] B. Hoeling, J. R. Yeh, T. Takekoshi, and R. J. Knize, Opt. Lett. **21**, 74 (1996).
[14] S. Aubin, E. Gomez, L. A. Orozco, and G. D. Sprouse, Rev. Sci. Instrum. **74**, 4342 (2003).
[15] W. Z. Zhao, J. E. Simsarian, L. A. Orozco, and G. D. Sprouse, Rev. Sci. Instrum. **69**, 3737 (1998).
[16] D. V. O'Connor and D. Phillips, *Time Correlated Single Photon Counting* (Academic, London, 1984).
[17] E. Gomez, F. Baumer, A. Lange, L. A. Orozco, and G. D. Sprouse (to be published).
[18] W. R. Johnson, Z. W. Liu, and J. Sapirstein, At. Data Nucl. Data Tables **64**, 279 (1996).
[19] J. E. Simsarian, W. Z. Zhao, L. A. Orozco, and G. D. Sprouse, Phys. Rev. A **59**, 195 (1999).
[20] M. Marinescu, D. Vrinceanu, and H. R. Sadeghpour, Phys. Rev. A **58**, R4259 (1998).
[21] C. E. Theodosiou, Bull. Am. Phys. Soc. **39**, 1210 (1994).
[22] E. Biémont, P. Quinet, and V. van Renterghem, J. Phys. B **31**, 5301 (1998).
[23] W. A. van Wijngaarden and J. Xia, J. Quant. Spectrosc. Radiat. Transf. **61**, 557 (1999).